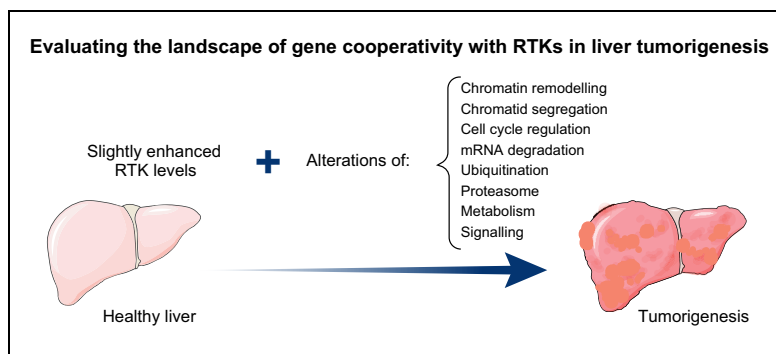


Evaluating the landscape of gene cooperativity with receptor tyrosine kinases in liver tumorigenesis using transposon-mediated mutagenesis

Graphical abstract



Highlights

- A transposon genetic screen uncovered 275 putative receptor tyrosine kinase cooperators for liver cancer.
- Most identified genes are also altered in patients with HCC.
- Receptor tyrosine kinase cooperators are regulators of a large spectrum of cellular functions.
- Enhanced receptor tyrosine kinase levels allow a broad range of mechanisms to initiate liver cancer.

Authors

Yannan Fan, Sehrish K. Bazai, Fabrice Daian, ..., Rosanna Dono, David A. Largaespada, Flavio Maina

Correspondence

flavio.maina@univ-amu.fr
(F. Maina)

Lay summary

Receptor tyrosine kinases (RTKs) are among signals frequently deregulated in patients with hepatocellular carcinoma and their deregulation confers essential biological properties to cancer cells. We have applied a genetic method to randomly mutate large numbers of genes in the context of a mouse model with increased RTK levels, predisposed to develop liver cancer. We identified mechanisms that accelerate tumour formation in cooperation with enhanced RTK levels. The wide array of cellular functions among these cooperators illustrates an extraordinary capability of RTKs to render the liver more vulnerable to additional alterations, by priming cells for tumour initiation.



Evaluating the landscape of gene cooperativity with receptor tyrosine kinases in liver tumorigenesis using transposon-mediated mutagenesis

Yannan Fan^{1, #}, Sehrish K. Bazai^{1, #}, Fabrice Daian¹, Maria Arechederra¹, Sylvie Richelme¹, Nuri A. Temiz², Annie Yim³, Bianca H. Habermann¹, Rosanna Dono¹, David A. Largaespada², Flavio Maina^{1, *}

¹Aix Marseille Univ, CNRS, Developmental Biology Institute of Marseille (IBDM) UMR 7288, Parc Scientifique de Luminy, Marseille, France; ²Department of Pediatrics, Masonic Cancer Center, University of Minnesota, Minneapolis, MN, USA; ³Computational Biology Group, Max Planck Institute of Biochemistry, Martinsried, Germany

Background & Aims: The variety of alterations found in hepatocellular carcinoma (HCC) makes the identification of functionally relevant genes and their combinatorial actions in tumorigenesis challenging. Deregulation of receptor tyrosine kinases (RTKs) is frequent in HCC, yet little is known about the molecular events that cooperate with RTKs and whether these cooperative events play an active role at the root of liver tumorigenesis.

Methods: A forward genetic screen was performed using *Sleeping Beauty* transposon insertional mutagenesis to accelerate liver tumour formation in a genetic context in which subtly increased MET RTK levels predispose mice to tumorigenesis. Systematic sequencing of tumours identified common transposon insertion sites, thus uncovering putative RTK cooperators for liver cancer. Bioinformatic analyses were applied to transposon outcomes and human HCC datasets. *In vitro* and *in vivo* (through xenografts) functional screens were performed to assess the relevance of distinct cooperative modes to the tumorigenic properties conferred by RTKs.

Results: We identified 275 genes, most of which are altered in patients with HCC. Unexpectedly, these genes are not restricted to a small set of pathway/cellular processes, but cover a large spectrum of cellular functions, including signalling, metabolism, chromatin remodelling, mRNA degradation, proteasome, ubiquitination, cell cycle regulation, and chromatid segregation. We validated 15 tumour suppressor candidates, as shRNA-mediated targeting confers tumorigenicity to RTK-sensitized cells, but not to cells with basal RTK levels. This demonstrates that the context of enhanced RTK levels is essential for their action in tumour initiation.

Conclusion: Our study identifies unanticipated genetic interactions underlying gene cooperativity with RTKs in HCC. Moreover, these results show how subtly increased levels of wild-type RTKs provide a tumour permissive cellular environment allowing a large spectrum of deregulated mechanisms to initiate liver cancer.

Lay summary: Receptor tyrosine kinases (RTKs) are among signals frequently deregulated in patients with hepatocellular carcinoma and their deregulation confers essential biological properties to cancer cells. We have applied a genetic method to randomly mutate large numbers of genes in the context of a mouse model with increased RTK levels, predisposed to develop liver cancer. We identified mechanisms that accelerate tumour formation in cooperation with enhanced RTK levels. The wide array of cellular functions among these cooperators illustrates an extraordinary capability of RTKs to render the liver more vulnerable to additional alterations, by priming cells for tumour initiation.

© 2018 European Association for the Study of the Liver. Published by Elsevier B.V. All rights reserved.

Introduction

Hepatocellular carcinoma (HCC) is among the most aggressive cancers, with an increasing incidence, and few therapeutic options.¹ The exceptional investments on -omics studies over the last decade have unveiled not only an impressive list of alterations, but also a high degree of molecular heterogeneity between patients with HCC.^{2,3} The uniqueness of HCC in its alterations and heterogeneity may explain how treatments effective in other cancers have largely failed when applied to HCC.⁴ Such context challenges the interpretation of -omics data, with the necessity to: i) determine which of these alterations are functionally relevant for tumorigenic properties, ii) distinguish sets of alterations with a tumour-boosting efficiency linked to specific patient subtypes or genetic contexts, and iii) elucidate how different combinatorial alterations can lead to equivalent vs. divergent fitness outcomes in cancer cells. The identification of functionally relevant signals, and of functional synergistic interactions between co-occurring events, is further complicated by the fact that some signals, although rarely

Keywords: Liver cancer; Mouse model; Tumour suppressors; Oncogenes; Receptor tyrosine kinases; Signalling; Hepatocellular carcinoma; HCC; Functional screening. Received 10 August 2018; received in revised form 20 November 2018; accepted 25 November 2018; available online 6 December 2018

* Corresponding author. Address: IBDM (Developmental Biology Institute of Marseille), 163 Avenue de Luminy, case 907, 13009 Marseille, France. Tel.: +33(0)4 91 26 97 69.

E-mail address: flavio.maina@univ-amu.fr (F. Maina).

Equal contribution.



mutated in HCC, are frequently activated in a high proportion of patients and are considered key regulators of tumorigenesis. This is the case, for example, for some receptor tyrosine kinase (RTK) pathway genes.^{4,5} The implication of deregulated RTK signalling in HCC is well established and RTK targeting agents are actively explored for combined therapies.⁶

The hepatocyte growth factor (HGF) receptor MET is one of the RTKs highly relevant in HCC. Although MET mutations are rare in HCC,⁷ MET is activated in close to 50% of cases,⁸ which correlates with poor prognosis.^{9–12} Overall, evidence implicating MET in HCC is sufficiently strong to have warranted several clinical trials of MET inhibitors.^{11,13,14} We have engineered a unique conditional transgenic mouse model (*R26^{stopMet}* mice)^{15–17} in which expression of wild-type (WT) MET can be slightly enhanced above its endogenous level in the liver (*Alb-R26^{Met}* mice). We demonstrated that an approximately 3-fold enhancement of MET levels in *Alb-R26^{Met}* mice is enough to perturb tissue homeostasis overtime in the liver, consecutively leading to tumour initiation and evolution into HCC.¹⁸ The clinical relevance of this liver cancer model is supported by studies showing that *Alb-R26^{Met}* HCCs: i) express MET levels comparable to those reported in ~20% of human HCC cases;¹⁸ ii) exhibit active, phosphorylated MET, as observed in close to 50% of patients with HCC;⁸ iii) model the so-called HCC “proliferative-progenitor” patient subclass;¹⁸ iv) while resistant to treatment with sorafenib, are sensitive to new synthetic lethal interactions we identified.¹⁸ We recently illustrated that *Alb-R26^{Met}* HCC are strikingly enriched in genes that are simultaneously overexpressed and hypermethylated in gene body CpG islands (CGIs), again similar to the “proliferative-progenitor” patient subclass.¹⁹ Such events are predictive of elevated levels of proto-oncogenes, which together act as an “oncogene module”.¹⁹ Therefore, the *Alb-R26^{Met}* mouse model is particularly suitable to identify non-predictable genetic interactions underlying gene cooperativity with RTKs during liver tumour initiation.

In the present study, we combined the Sleeping Beauty (SB) transposon mutagenesis system²⁰ with *Alb-R26^{Met}* livers, as an approach to accelerate liver tumour formation. Upon characterisation of transposon insertion sites in the resulting tumours, we report the identification of 275 genes as putative cooperators with RTKs in tumorigenesis and show that most of them are altered in patients with HCC. We identified co-occurring gene alteration events that are also present in patients with HCC. Bioinformatic analyses illustrated that the *Alb-R26^{Met}-transposon* genes exert distinct functions in cells. We established the tumour-suppressive capability of 15 candidates belonging to distinct cellular mechanisms. We demonstrated that the context of enhanced RTK levels is essential, as down-regulation of these tumour suppressors in WT cells without enhanced RTK levels does not confer tumorigenicity. Collectively, our results show how subtly increased levels of WT RTKs provide a permissive context allowing multiple deregulated mechanisms to initiate liver cancer.

Materials and methods

For further details regarding the materials and methods used, please refer to the [CTAT table](#) and [supplementary information](#).

Genomic DNA processing, pyrosequencing, and transposon integration data analyses

Ligation-mediated PCR with genomic DNA from 248 tumours, pyrosequencing data and findings processing was performed as previously reported.²¹

Co-occurring events in *Alb-R26^{Met}*-transposon screen and in patients with HCC

Co-occurrence analysis was performed to identify genes frequently mutated in the *Alb-R26^{Met}-transposon* screen at a higher frequency than expected by chance.²² A co-occurrence tumour mutation contingency table was built to calculate co-occurrence p values by performing a Fisher's exact test on each couple of *Alb-R26^{Met}* genes. We applied a Benjamini-Hochberg false discovery rate correction and a threshold of significance was established at <0.05, leading to the identification of 119 pairs of co-occurring events (Table S5). Several genes were also identified as co-occurrences in patients with HCC based on concurrent differential expression (Log2 fold change >1 or <-1). We then built a contingency table, performed Fisher's exact test on each gene couple, then applied a Benjamini-Hochberg FRD correction using a significance level of <0.05 (Table S5).

Western blots

Protein extracts from livers, tumours, *immorto-WT* and *immorto-R26^{Met}* hepatocytes were processed for western blots, as previously described.^{8,16,23}

Cell cultures

Primary culture of E15.5 WT and *R26^{Met}* embryonic hepatocytes were established as previously described.^{24–26} Hepatocytes were immortalized by adapting a procedure previously reported.²⁷

Results

SB-induced mutagenesis accelerates tumour development triggered by subtle enhancement of WT MET levels

To search for genes whose mutations may accelerate tumorigenicity by slightly enhanced WT MET levels,¹⁸ we combined the *Alb-R26^{Met}* mice with the SB transposon mutagenesis system in which conditional expression of the SB transposase leads to transposon (*T2/onc2*) mobilization in the liver (Fig. 1A, Fig. S1A,B). As the SB has the tendency to favour transposon jumping adjacent to the donor concatemers, a phenomenon known as “local hopping”, we performed our screen using *T2/onc2-6070* and *T2/onc2-6113* lines, which carry transposon concatemers on chromosome 4 and 1, respectively. The resulting *Alb:cre-T2/onc2-R26^{SB/+}* mice are referred to as “Triple^{tg}” (Fig. 1A). We confirmed that *Alb-cre*-mediated excision of the stop cassette in the liver simultaneously leads to conditional expression of MET^{tg} and SB transposase in *Alb:cre-T2/onc2-R26^{SB/Met}* livers (referred to as “Quadruple^{tg}”; Fig. 1A-C). *Quadruple^{tg}* started to develop tumours around 30 weeks of age, a stage when tumours are still not detected in the *Alb-R26^{Met}* genetic setting as tumorigenesis starts around 40–48 weeks¹⁸ (*Quadruple^{tg}* with *T2/onc2-6070*: 51%; *Quadruple^{tg}* with *T2/onc2-6113*: 64%; Fig. 1E, F, Table S1). In contrast, only 1

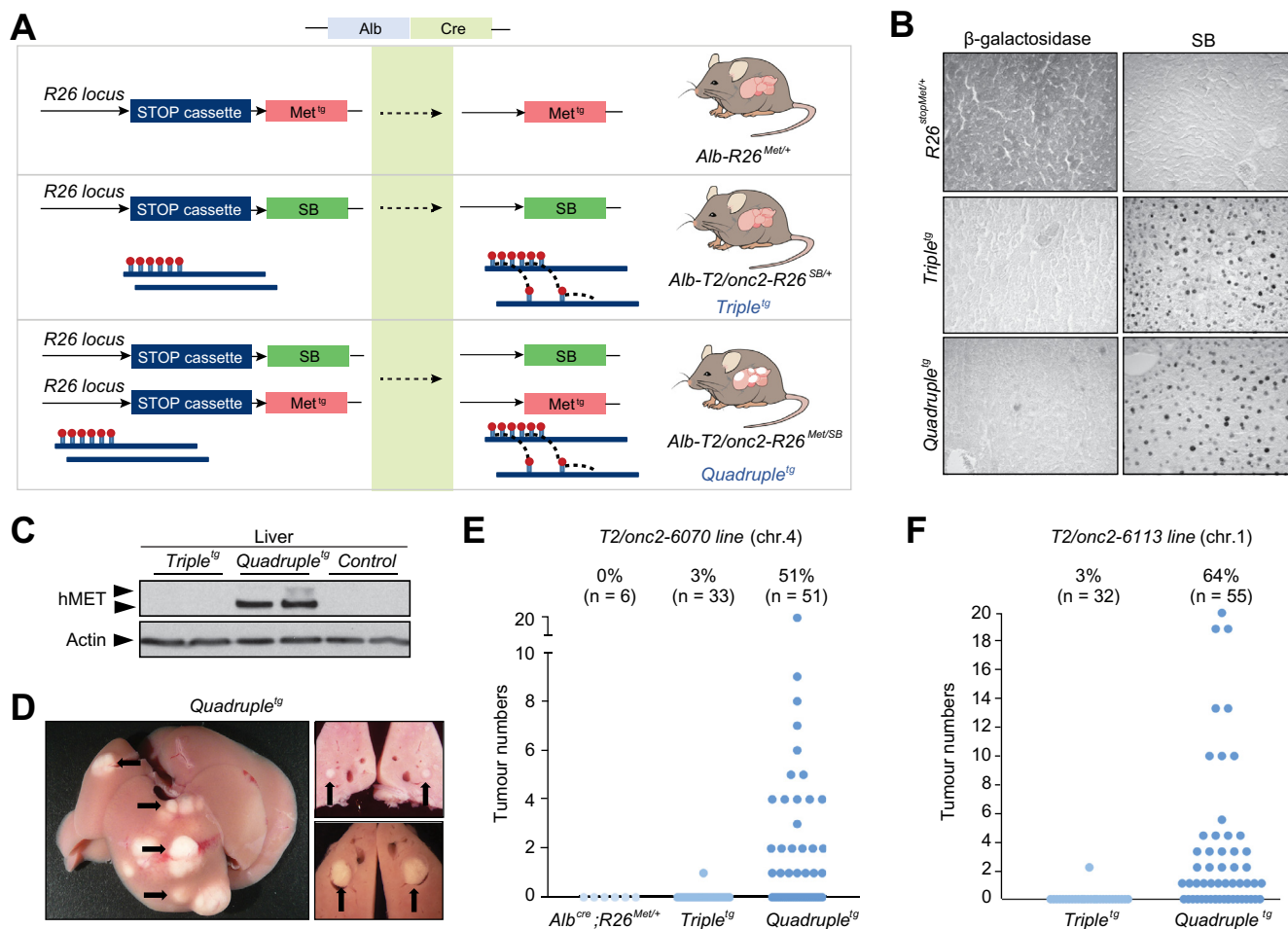


Fig. 1. Genetic settings employed for the *Alb-R26^{Met}*-transposon screen. (A) Schematic representation of the 3 genetic settings employed for the SB transposon mutagenesis screen. Concerning the *T2/onc* transgenics, a concatemer of transposons is present on chromosome 4 (6070 line) or chromosome 1 (6113 line). (B) Immunohistochemical analysis reporting β -galactosidase and SB transposase expression in the indicated genetic settings. (C) Western blot analysis of total protein extracts from *Triple^{tg}*, *Quadruple^{tg}*, and control livers. Note MET^{tg} expression specifically in *Quadruple^{tg}* (detected by anti-human MET antibodies). Actin was used as a loading control. (D) Examples of liver tumours in *Quadruple^{tg}* (arrows). Tumour size ranged from 1 to 4 mm diameters (Table S1). Example of multiple tumours (left) or single small tumours within the liver lobes (right) are shown. (E,F) Tumour formation in *Alb-R26^{Met}*, *Triple^{tg}*, *Quadruple^{tg}* at 30 weeks of age. Data correspond to *T2/onc2-6070* (E) and *T2/onc2-6113* (F) lines. Each dot corresponds to a mouse. The percentage (and numbers) of mice developing liver tumours is indicated. SB, Sleeping Beauty. (This figure appears in colour on the web.)

Triple^{tg} in each *T2/onc2* line developed tumours (Fig. 1D-F, Fig. S1C Table S1). Thus, irrespective of the initial location of the transposon concatemers, the ideal context in which only *Quadruple^{tg}* develop tumours at 30 weeks of age offered the possibility to unambiguously search for alterations underlying putative genetic interactions with WT RTKs during tumour initiation.

Identification of putative cancer-related genes accelerating tumorigenesis by slightly enhanced MET levels

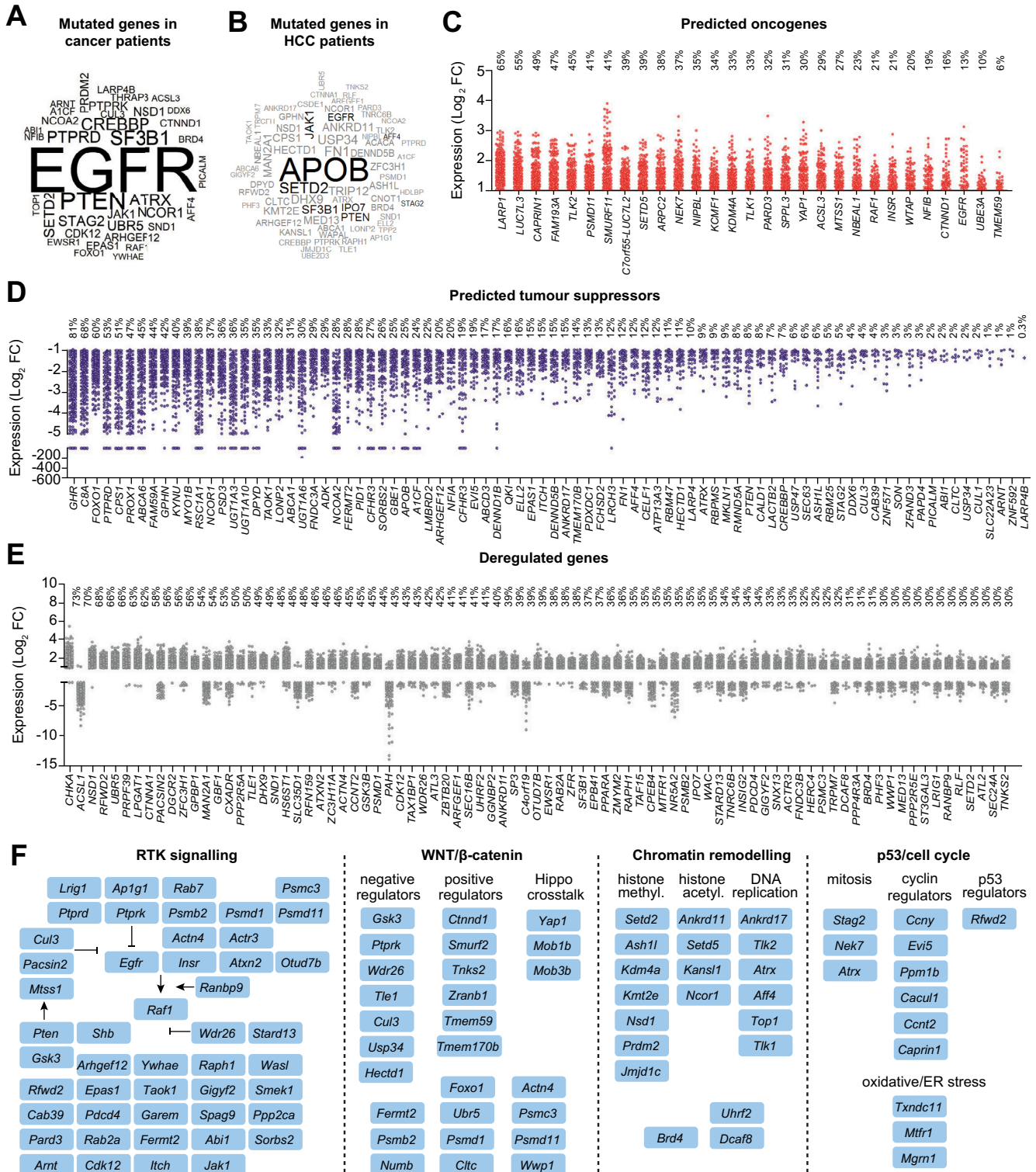
A total of 248 liver tumours were collected from *Quadruple^{tg}* (with either *T2/onc2-6070* or *T2/onc2-6113* line) and successfully processed for pyrosequencing analysis. The procedure involved DNA barcoding of each tumour to pool and process them simultaneously, as previously reported.²¹ TAPDANCE analysis identified ~47,000 non-redundant regions of transposon insertion, and defined 312 common insertion sites²⁸ in tumour samples from *Quadruple^{tg}*. We then annotated these common insertion sites to the nearest mouse gene, thereby identifying 275 genes (named as *Alb-R26^{Met}*-transposon genes; defined by the identification of at least 8 insertions in at least 8 libraries; Fig. S1D).

Based on sequencing read counts for each *Alb-R26^{Met}*-transposon gene, transposon insertions occurred in more than 10% of tumours for 32 genes, suggesting that these genes are among the most frequent regulators of liver tumour initiation (Fig. S1D,E, Fig. S2, Table S2). We positioned the orientation of transposon integration in each gene and examined orientation biases of SB insertions to predict their effects on genes (Fig. S1F, Table S2). By integrating these data with the location and the distribution of transposon insertions within the gene locus, we predicted putative effects on the *Alb-R26^{Met}*-transposon genes. For 103 genes, insertions were randomly distributed through the gene and occurred in both orientations or with a bias toward antisense, indicating that the contribution of these genes to tumorigenesis likely resulted from loss of gene function. These genes were thus predicted as putative tumour suppressors. For 29 genes, transposon insertions were most likely compatible with gain-of-function expression of full length or truncated forms. Thus, these genes were predicted as putative oncogenes. For the remaining 143 genes, orientation and position of transposon insertions could predict either gene disruption or generation of truncated forms.

Most of the putative cancer-related genes identified in the *Alb-R26^{Met}* genetic setting are deregulated in a proportion of patients with HCC

We next determined the relevance of *Alb-R26^{Met}-transposon* genes to human cancer and particularly to HCC pathogenesis. For comparisons between mouse and human data, the corre-

sponding human orthologues to the *Alb-R26^{Met}-transposon* genes were determined. Accordingly, 267 mouse genes were matched to the corresponding human gene (99/103 predicted tumour suppressors, 29/29 predicted oncogenes, 139/143 genes for which the effect of transposon insertions was uncertain; Fig. S3A, Table S3). By querying the Catalogue of Somatic



Mutations in Cancer (COSMIC) databases, we identified 41 genes frequently mutated in human cancer ($p = 1.80E-20$, 719 Census genes, hypergeometric-test; Fig. 2A, Table S3).

Next, we explored how alterations of *Alb-R26^{Met}-transposon* genes are associated with HCC pathogenesis using The Cancer Genome Atlas (TCGA) database. We analysed both expression changes (data available for 371 patients) and the presence of mutations (data available for 363 patients). Concerning mutations, we found that some of the *Alb-R26^{Met}-transposon* genes are also mutated in patients with HCC³ (Fig. 2B, Table S3). Overall, 71 (26%) of *Alb-R26^{Met}-transposon* genes are mutated in at least 1% of HCC patients and 218 (79%) genes in at least 1 HCC patient (Table S3). Concerning changes in expression levels, data were available for 251 out of the 267 orthologues human genes (Fig. S3A, Table S3). All the 251 *Alb-R26^{Met}-transposon* human orthologue genes are differentially expressed in at least a proportion of the 371 patients with HCC who were analysed (Table S3). In particular, the 29 predicted oncogenes are upregulated in a proportion of patients with HCC, ranging from 6% to 65% (Fig. 2C, Table S3). Concerning the 86 predicted tumour suppressors, a large set of patients with HCC had consistently decreased expression levels (Fig. 2D, Table S3). In particular, 66 predicted tumour suppressors are downregulated in at least 6% of human HCCs, ranging up to 81% for GHR (Fig. 2D). We also analysed the expression levels of the 136 *Alb-R26^{Met}-transposon* genes, for which we could not predict whether they acted as tumour suppressors or oncogenes in the *Alb-R26^{Met}* genetic setting. Remarkably, a large set of human HCC is characterised by deregulation of these genes, with several of them predominantly either upregulated or downregulated (Fig. 2E, Fig. S3B, Table S3).

We then explored whether altered expression levels of the *Alb-R26^{Met}-transposon* genes correlate with *MET* levels in patients with HCC. Concerning predicted oncogenes, there is a striking positive correlation between their overexpression and high *MET* expression levels (Fig. 3A,B, Table S3). For predicted tumour suppressors, we instead found that their downregulation predominantly occurred in patients with HCC and low *MET* levels (Fig. 3A,C, Table S3). The same types of correlation characterised those genes for which the effect of transposon insertions was uncertain: whereas a large proportion of them are predominantly overexpressed in patients with HCC and high *MET* levels, the others are mainly downregulated in patients with low *MET* levels (Fig. S3, Table S3). Thus, although our screen in mice shows that *MET* can trigger tumorigenesis in cooperation with targeted tumour suppressors, in patients with HCC and enhanced *MET* levels, tumorigenesis can occur even without

major deregulation of this tumour suppressor set. It is tempting to speculate that *MET* might alleviate the need to lower tumour suppressor levels, for example by increasing oncogene levels. Furthermore, the intriguing correlation between high levels of predicted oncogenes and *MET* in patients with HCC is reminiscent of a novel mechanism we recently discovered, in which *MET*-driven HCC is characterised by high dosage of oncogenes through CGI hypermethylation in the gene body.¹⁹

Recent studies using human HCC databases have identified 5 major signalling pathways commonly altered in human HCC: PI3K/Ras signalling (herein termed RTK signalling); WNT/ β -catenin, chromatin remodelling, p53/cell cycle, and oxidative/endoplasmic reticulum stress.^{29,30} To corroborate the relevance of *Alb-R26^{Met}-transposon* genes in HCC biology, we analysed which of them belong to these 5 major signalling pathways and identified 96 genes. Intriguingly, the list of *Alb-R26^{Met}-transposon* genes is enriched in those involved in RTK signalling (48 genes), WNT/ β -catenin (27 genes), chromatin remodelling (20 genes), rather than in p53/cell cycle (10 genes) and oxidative/endoplasmic reticulum stress (3 genes; Fig. 2F, Table S4). Consistently, we found activation of RTK and WNT signalling in a set of transposon tumours carrying insertions in genes acting as regulators of these pathways (Fig. S5). Thus, tumorigenesis modelled by our transposon strategy appears to occur through genetic alterations of pathways frequently perturbed in human HCC.

Co-occurring events discovered in the *Alb-R26^{Met}* genetic setting arise in a proportion of patients with HCC

We searched for genes co-mutated at a higher frequency than expected by random events and identified 119 events of co-occurrence (Fig. 4, Table S5). By analysing the frequency linking each of these genes, we reconstituted nodes of interactions, identifying 4 co-occurring subnetworks of associated commonly occurrences (Fig. 4, Table S5). Beside these, 11 co-occurrences not related to the 4 subnetworks were identified (Fig. 4). Strikingly, the largest co-occurring subnetwork involves 43 genes, among which the genes are involved in one or multiple types of co-occurrences (for a total of 62 co-occurrences; Fig. 4, Table S5). This large subnetwork comprises genes belonging to several pathways, including RTK signalling, chromatin remodelling, transcriptional regulation, WNT/ β -catenin, ubiquitination.

Intrigued by these findings, we asked whether co-occurring events identified in the *Alb-R26^{Met}* genetic setting could also be recognized in patients with HCC. Remarkably, 51 co-occurrences (43%) were identified in at least 10% of HCC patients

Fig. 2. Cross-species comparison implicates the *Alb-R26^{Met}-transposon* genes in HCC pathogenesis and a proportion of them in human cancers. (A) Word-cloud diagram reporting the 41 *Alb-R26^{Met}-transposon* genes frequently mutated in human cancer according to the COSMIC Census gene databases (Table S3). (B) Word-cloud diagram reporting the *Alb-R26^{Met}-transposon* genes mutated in patients with HCC. The 9 genes significantly mutated in human HCC are indicated in black (p value <0.05). The 70 genes mutated in more than 1% of HCC patients are indicated in grey (Table S3). In A and B, the size of each gene name is representative of the percentage of patients with mutations in the corresponding genes. (C-E) RNA-seq data from human HCC patients were queried for alterations in *Alb-R26^{Met}-transposon* gene expression (Table S3). (C) Scatterplot depicting HCC patients with upregulation (Log_2 FC >1) of predicted oncogenes according to effects of transposon insertion. (D) Scatterplot depicting HCC patients with downregulation (Log_2 FC <-1) of predicted tumour suppressors according to effects of transposon insertion. (E) Scatterplot depicting HCC patients with deregulation (Log_2 FC >1 and Log_2 FC <-1) of genes for which transposon insertions did not allow unambiguous effect prediction. Only *Alb-R26^{Met}-transposon* genes deregulated in at least 30% of HCC patients are reported. The other genes are shown in Fig. S2B. (F) *Alb-R26^{Met}-transposon* genes belonging to the 5 major pathways reported to be altered in HCC patients:^{29,30} RTK signalling, WNT/ β -catenin, chromatin remodelling, p53/cell cycle, and oxidative/endoplasmic reticulum stress. Note an enrichment in genes participating to RTK signalling, WNT/ β -catenin, and chromatin remodelling. The RTK core pathway includes genes either regulating or participating to the RTK signalling. Some positive and negative regulations are indicated. Concerning the WNT/ β -catenin, most genes are organised as negative or positive regulators; genes belonging to the WNT/Hippo pathway crosstalk are also highlighted. Concerning chromatin remodelling, most genes are grouped into regulators of histone methylation, histone acetylation, DNA replication. Concerning p53/cell cycle, genes are organised according to their implication in mitosis, cyclin, p53 regulators. FC, fold change; HCC, hepatocellular carcinoma; RTK, receptor tyrosine kinase. (This figure appears in colour on the web.)

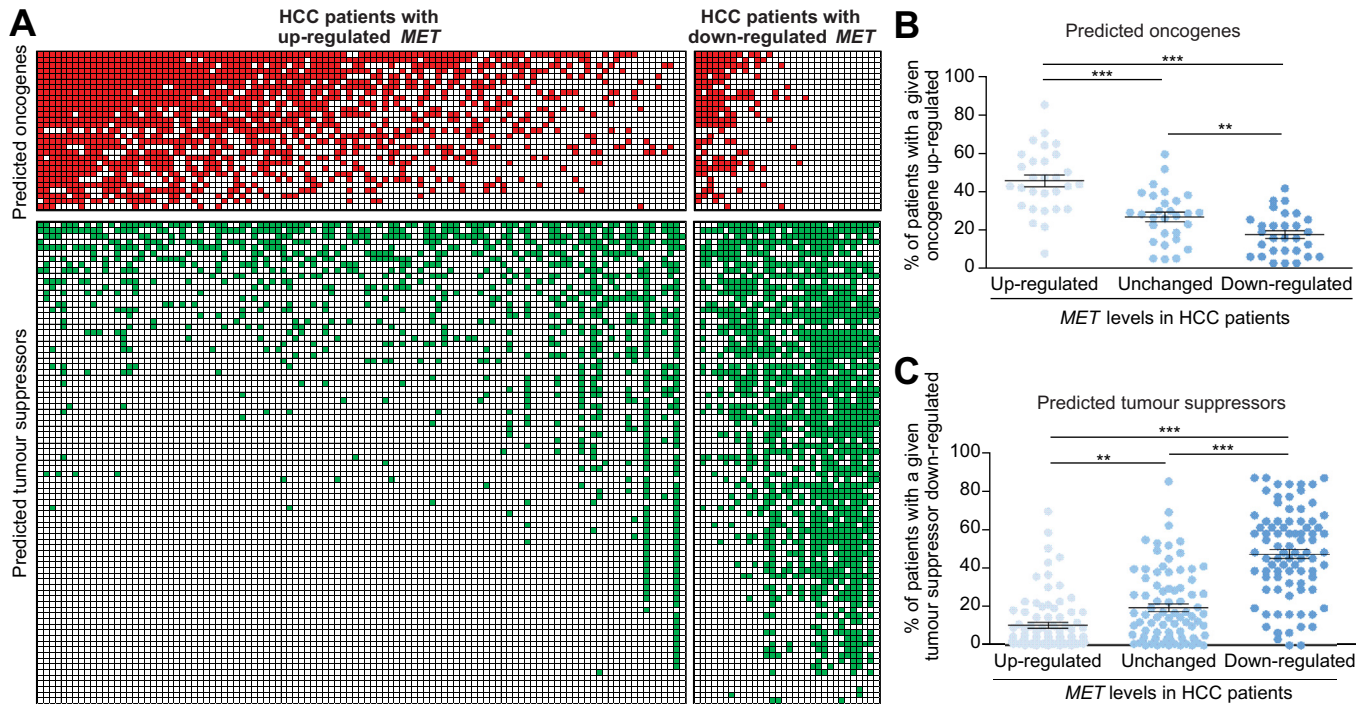


Fig. 3. Predicted *Alb-R26^{Met}*-transposon oncogenes are predominantly upregulated in HCC patients with high *MET* levels, whereas predicted tumour suppressors are predominantly downregulated in HCC patients with low *MET*. (A) Heat-map reporting expression levels of predicted oncogenes and tumour suppressors (rows) in individual patients with HCC (columns; organised according to the higher number of patients with upregulated oncogenes or downregulated tumour suppressors). Red: upregulated oncogenes; green: downregulated tumour suppressors. (B,C) In the graphs, each dot corresponds to a given (B) oncogene or (C) tumour suppressor, and their position to the percentage of patients in which the gene is upregulated or downregulated, respectively. Significant differences (unpaired Student t-test) are indicated: ***p* < 0.01; ****p* < 0.001. HCC, hepatocellular carcinoma. (This figure appears in colour on the web.)

(Fig. 4, Table S5). These co-occurrences included those belonging to the large co-occurring network as well as all those composing one of the 3 subnetworks we identified. Thus, a SB transposon mutagenesis screen in the *Alb-R26^{Met}* liver cancer mouse model identifies transcriptomic and genetic alterations as well as co-occurring events in patients with HCC. The co-occurrences may reflect possible synergistic effects between genes, increasing the likelihood that each of them ensures the tumorigenic process.

The *Alb-R26^{Met}*-transposon genes identify multiple enriched pathways with distinct functions in cells

We carried out an analysis of the *Alb-R26^{Met}*-transposon genes using ReactomePA databases and found that several cancer-related pathways are significantly enriched, such as WNT, B Cell Receptor, RTK signalling (Fig. S6, Table S6). To define putative biological functions of *Alb-R26^{Met}*-transposon genes, we applied Database for Annotation, Visualisation, and Integrated Discovery (DAVID). These analyses allowed us to demonstrate an enrichment in genes related to ubiquitination, signalling pathway, metabolism, transcription, cell motility, and cancer (Table S6). To get further insights into which molecular and cellular functions the *Alb-R26^{Met}*-transposon genes belong to, we performed additional enrichment analyses by applying the Enrichr tool. Concerning signalling pathways, we found an enrichment of the RTK signalling core pathway (e.g. Focal Adhesion-PI3K-mTOR, RTK effectors), TGFβ, WNT, NF-κB, immune signalling (e.g. IL-6, IL-7), Delta-Notch, histone modification, metabolism, RNA processing, proteasome degradation, ubiquitination (Fig. 5A, Table S6). The *Alb-R26^{Met}*-transposon genes also identify kinases based on their phosphorylation tar-

gets or the set of genes they are coexpressed with (Fig. 5B, Table S6). Similarly, the *Alb-R26^{Met}*-transposon genes also identify a number of kinases recognizable by signatures of gene perturbations (upregulation/downregulation) following kinase knockdown (Fig. 5C, Table S6). Concerning transcription, several transcription factors were enriched for either co-occurring or interacting with sets of *Alb-R26^{Met}*-transposon genes (Fig. 5D, Table S6). Concerning human disease, most enriched diseases are different types of cancer (with liver cancer ranked third), fatty liver disease, hyperinsulinism, and hyperglycaemia (Fig. 5E, Table S6). Several *Alb-R26^{Met}*-transposon genes are computational predicted target of microRNA (Table S6). Next, we searched for associations between the *Alb-R26^{Met}*-transposon genes using STRING, which represents interactions (known or predicted) between genes (265/275 genes were found in the STRING database). Remarkably, a projection of *Alb-R26^{Met}*-transposon genes onto the STRING protein-protein interaction network revealed that most of them are part of a network of interactions (179; Fig. 6, Fig. S7,S8, Table S6). Beside this large network, 4 associations were also identified (1 with 3 genes and 3 with 2 genes; Fig. 6, Fig. S7,S8). These analyses illustrate how the *Alb-R26^{Met}*-transposon genes are highly connected. Deregulation of these genes may propagate throughout the network, thus perturbing multiple processes. Collectively, the SB transposon mutagenesis in the *Alb-R26^{Met}* genetic setting highlighted a large spectrum of pathways as potential acting modes for tumorigenicity. Moreover, these analyses uncovered some genes with a putative implication in cancer, for which a biological function and/or relevance in cancer was largely unknown (Table S2).

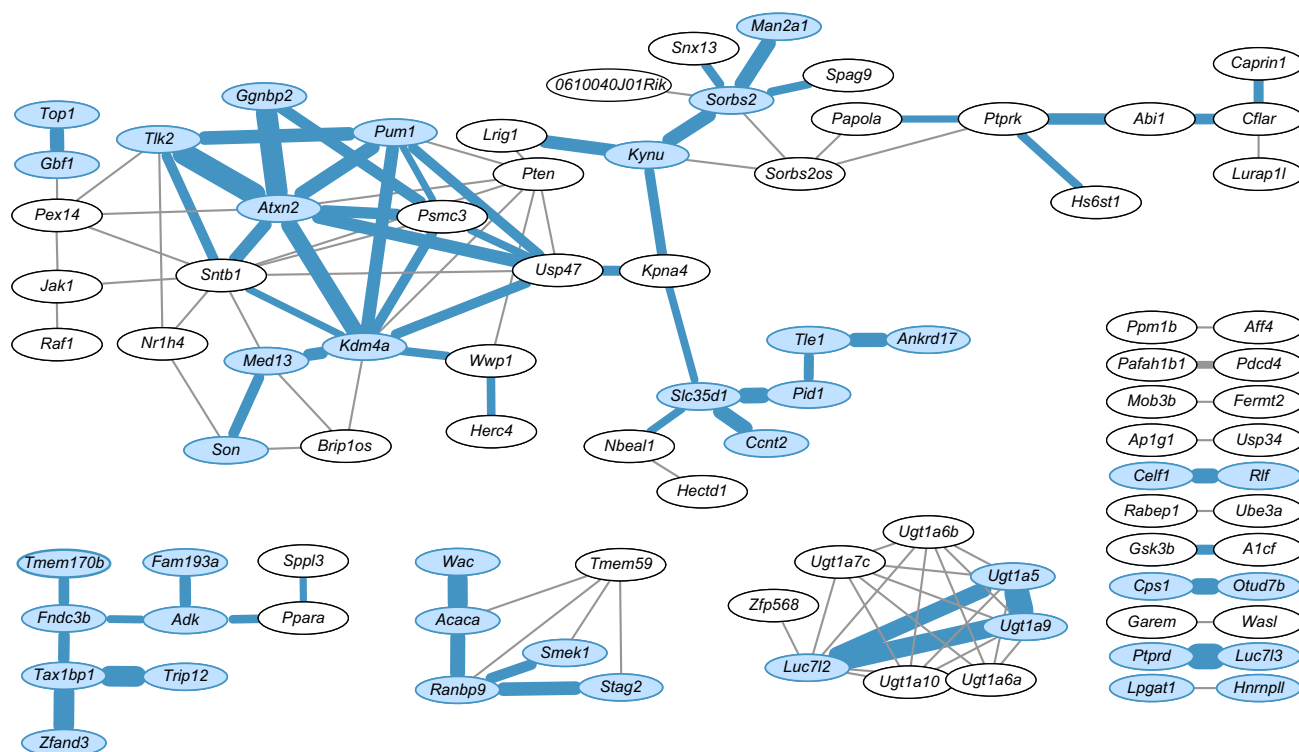


Fig. 4. Co-occurring events in the *Alb-R26^{Met}*-transposon screen can be grouped into interacting networks, with a large proportion present in HCC patient subsets. Based on pairwise comparisons between each *Alb-R26^{Met}*-transposon genes and Fisher’s exact test, 119 co-occurrences were identified in the *Alb-R26^{Met}* liver cancer model. Beside the 11 co-occurring events concerning only 2 genes (right), a large network (composed by 43 genes) and 3 subnetworks were spotted (Table S5). Among the 4 co-occurring subnetworks, one of them includes *Zfp568*, *Luc712* together with several *Ugt1a* family members, encoded by a single gene locus (Fig. S12). 51 co-occurrences are present in at least 10% of patients with HCC, shown in the figure with blue interconnecting lines in which the thickness between 2 genes represents the percentage of co-occurring events in patients. Co-occurring alterations in at least 15% of human HCCs are indicated in blue (Table S5). HCC, hepatocellular carcinoma. (This figure appears in colour on the web.)

Comparison to other SB-induced liver cancer models identifies a set of ‘putative RTK-specific genes’

Next, we assessed the level of specificity in gene cooperation with enhanced MET levels by comparing the *Alb-R26^{Met}*-transposon genes with those identified in other liver SB screens: *p53^{mut}*²¹ *Myc^{over}*³¹ *HBV^{tg}*³² chemically induced chronic liver injury,³³ hepatic steatosis,³⁴ epithelial-mesenchymal transition.³⁵ Among the 275 *Alb-R26^{Met}*-transposon genes, 226 (82%) were found in one or more of the SB screen cohorts. These genes are likely to be relevant to liver cancer, with a competence to cooperate with other sensitizing mutations (Fig. 7A, Table S7). Consistently, some of them have been functionally validated for their participation as tumorigenic drivers in other settings. Interestingly however, 49 genes were unique to our *Alb-R26^{Met}*-transposon cohort (Fig. 7B, Table S7). We next used bioinformatics to assess whether these genes belong to specific molecular and biological processes by applying the Enrichr tool. Several kinases are enriched according to their co-expression with sets of ‘putative RTK-specific genes’ (Fig. 7C, Table S7). These ‘putative RTK-specific genes’ also identify several kinases recognizable by signatures of gene perturbations (upregulation/downregulation) following kinase knockdown (Fig. 7D, Table S7). Among enriched kinases, are those belonging to signalling pathways such as MAPK, Insulin, and NF-κB. Concerning transcription, several transcription factors are enriched according to either co-expression or to consensus targets with sets of ‘putative RTK-specific genes’ (Fig. 7E, Table S7). Among the top enriched transcription factors are those related to WNT/βcatenin and stemness (e.g. *CHD1*, *CHD2*, *SMAD4*, *FOXO1*, *KLF4*, *TCF3*,

SOX2). Enrichments also included methylated/unmethylated CpG binding-transcription factors as well as genes involved in chromatin modifications. Concerning biological processes, enrichments include post-translational modifications, ubiquitination, regulation of transcription and splicing, chromatin modification, and metabolism (Fig. 7F, Table S71). Thus, the ‘putative RTK-specific’ *Alb-R26^{Met}*-transposon genes also exert distinct functions in cells and are part of multiple regulatory networks.

Functional validation of a set of tumour suppressors uncovers the promiscuous capability of RTK to cooperate with distinct genes during liver tumour initiation

The broad spectrum of cellular regulators highlighted through bioinformatic analysis may indicate that a context with subtly enhanced RTK levels can cooperate with alterations of different types of mechanisms for liver tumorigenesis. Therefore, we designed a functional validation screen aimed at assessing whether a context of enhanced WT MET levels permits altered regulators of distinct cellular mechanisms to initiate transformation. For this screen, we selected 16 predicted tumour suppressor candidates (Fig. S9) acting as regulators of distinct functions: metabolism (*Adk*), cell cycle (*Cacul1*), proteasome (*Ddi2*), mRNA degradation (*Ddx6*), chromatin remodelling (*Kansl1*, *Kmt2e*, *Ncor1*), signalling (*Ppp6r3*, *Ptpkd*, *Sorbs2*), chromatin segregation (*Stag2*), ubiquitination (*Usp34*, *Usp47*), transcription (*Zfand3*). We also selected 2 genes whose function is largely unknown: *Lrch3* and *Wbp1L*. For 11 genes, mutations and downregulation in expression levels were observed in human HCC (Table S3).

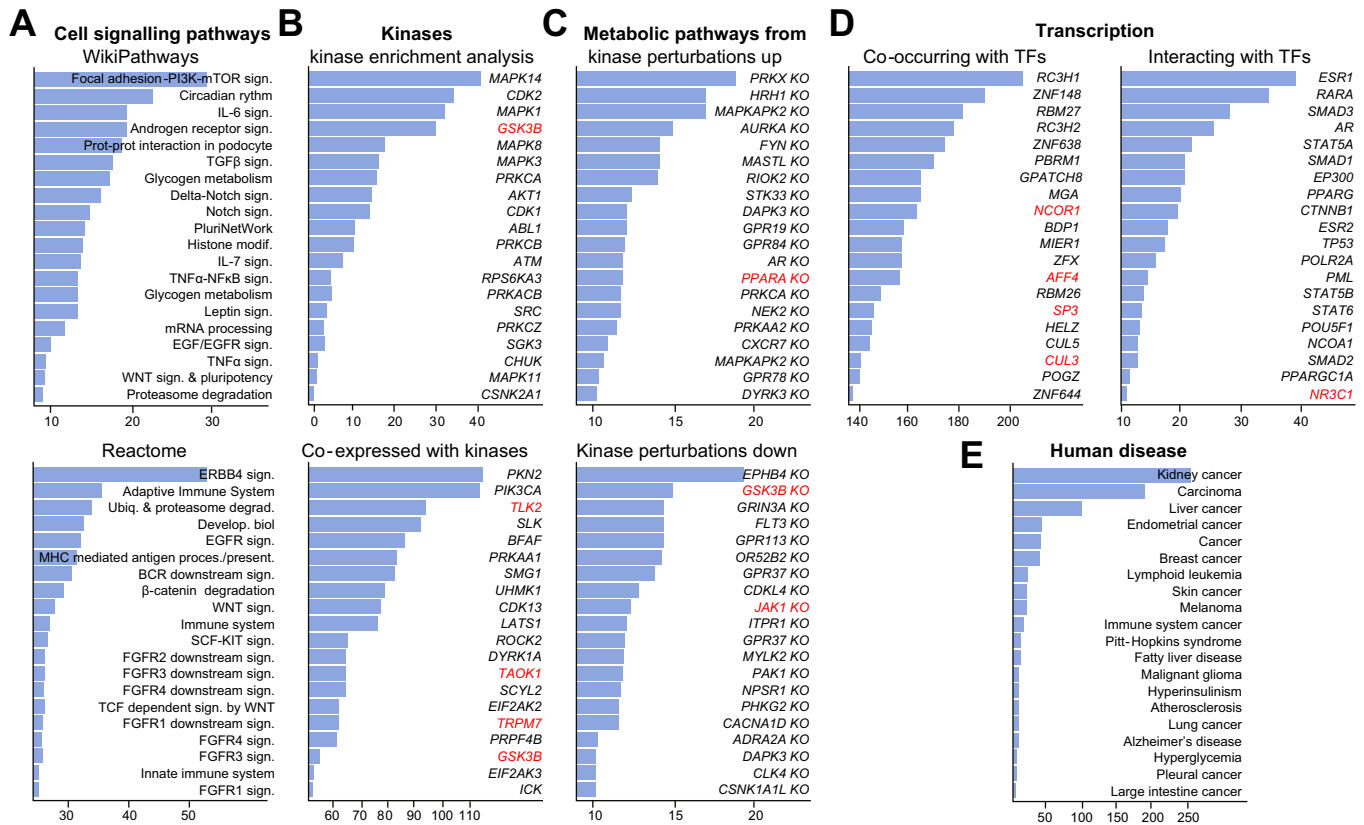


Fig. 5. Multiple signalling and transcription networks are enriched by the *Alb-R26^{Met}*-transposon genes. Enrichment analyses by applying the Enrichr tool. (A) Histogram reporting the cell signalling pathway enrichment, ordered according to the combined score (top: WikiPathways database; bottom: Reactome database). (B) Histogram reporting the kinases identified based on their phosphorylation targets among identified genes (top: Kinase Enrichment Analysis, KEA database) or the set of identified genes they are coexpressed with (bottom: Coexpressed with kinases, ARCHS4 kinases Coex database). (C) Histogram reporting kinases recognizable by signatures of gene perturbations (upregulation/downregulation) following kinase knockdown. (D) Histogram reporting TFs enriched for either co-occurring (left: Enrichr submission TF-Gene Co-occurrence database) or interacting (right: TF protein-protein interaction database) with sets of *Alb-R26^{Met}*-transposon genes. Additional analyses based on ChEA, Encode & ChEA consensus TFs from ChIP-X, and ARCHS4 TFs coexp databases are reported in Table S6. (E) Histogram reporting enrichment of human diseases (Jensen Diseases database). (B,C,D) Enriched kinases and TFs belonging to the *Alb-R26^{Met}*-transposon genes are indicated in red. In all panels, enrichments are ordered according to combined scores (values are indicated on the x axis). TF, transcription factor. (This figure appears in colour on the web.)

First, we generated hepatocytes from E15.5 *R26^{Met}* livers (as well as from E15.5 WT livers as control) and immortalized them with a SV40 Large T antigen (*immorto-R26^{Met}* and *immorto-WT* hepatocytes; Fig. 8A), a strategy employed in previous studies.³¹ The capacity of both *immorto-R26^{Met}* and *immorto-WT* hepatocytes to grow in arginine-free culture conditions confirmed their liver origin. These *immorto-R26^{Met}* hepatocytes are not tumorigenic, as they do not form tumours in immune-compromised mice and colonies in anchorage-independent growth assays (Fig. S10A,B). Thus, in this cellular setting, the enhanced WT MET expression levels, although not sufficient on its own, may prime cells towards tumorigenesis by providing a sensitized genetic background for cooperativity with additional genetic alterations. Western blot analyses revealed an approximately 3-fold increase in MET expression levels in *immorto-R26^{Met}* hepatocytes compared to *immorto-WT* controls (Fig. 8B), as previously reported in E15.5 primary embryonic hepatocytes and in *Alb-R26^{Met}* HCC.¹⁶ Qualitative analysis revealed that in both cellular systems, phosphorylation of MET and downstream signals is conditioned by HGF stimulation (Fig. 8C), coherent with results in E15.5 primary embryonic hepatocytes.^{16,18}

Next, we explored functionality of the 16 putative tumour suppressor candidates by downregulating their mRNA expression levels in *immorto-R26^{Met}* hepatocytes using the shRNA targeting strategy (Fig. 8A). For most candidate genes, we tested 2 to 5 different shRNA targeting sequences and chose the most efficient shRNA for functional validation studies (Fig. S10C, Table S8). Transfected cells were then used to assess whether mRNA downregulation of candidate genes conferred in vitro and in vivo tumorigenicity to *immorto-R26^{Met}* hepatocytes, thus qualifying them as functional tumour suppressors. To assess cell tumorigenicity in vitro, we performed anchorage-independent growth assays. Results show for each tested gene, the relative increase in the capacity of *immorto-R26^{Met}* hepatocytes to form colonies compared to cells either non-transfected or transfected with an shRNA control sequence (Fig. 8D). These results were further strengthened by xenograft studies in nude mice. For 15 of the 16 candidate genes, shRNA-mediated mRNA downregulation conferred in vivo tumorigenicity to *immorto-R26^{Met}* hepatocytes (Fig. 8E, Fig. S11A). Outcomes also highlighted differences in ‘fitness’ (tumour size), possibly reflecting varying potential of these tumour suppressors to cooperate with MET when downregulated. The only exception concerned *immorto-R26^{Met}* hepa-

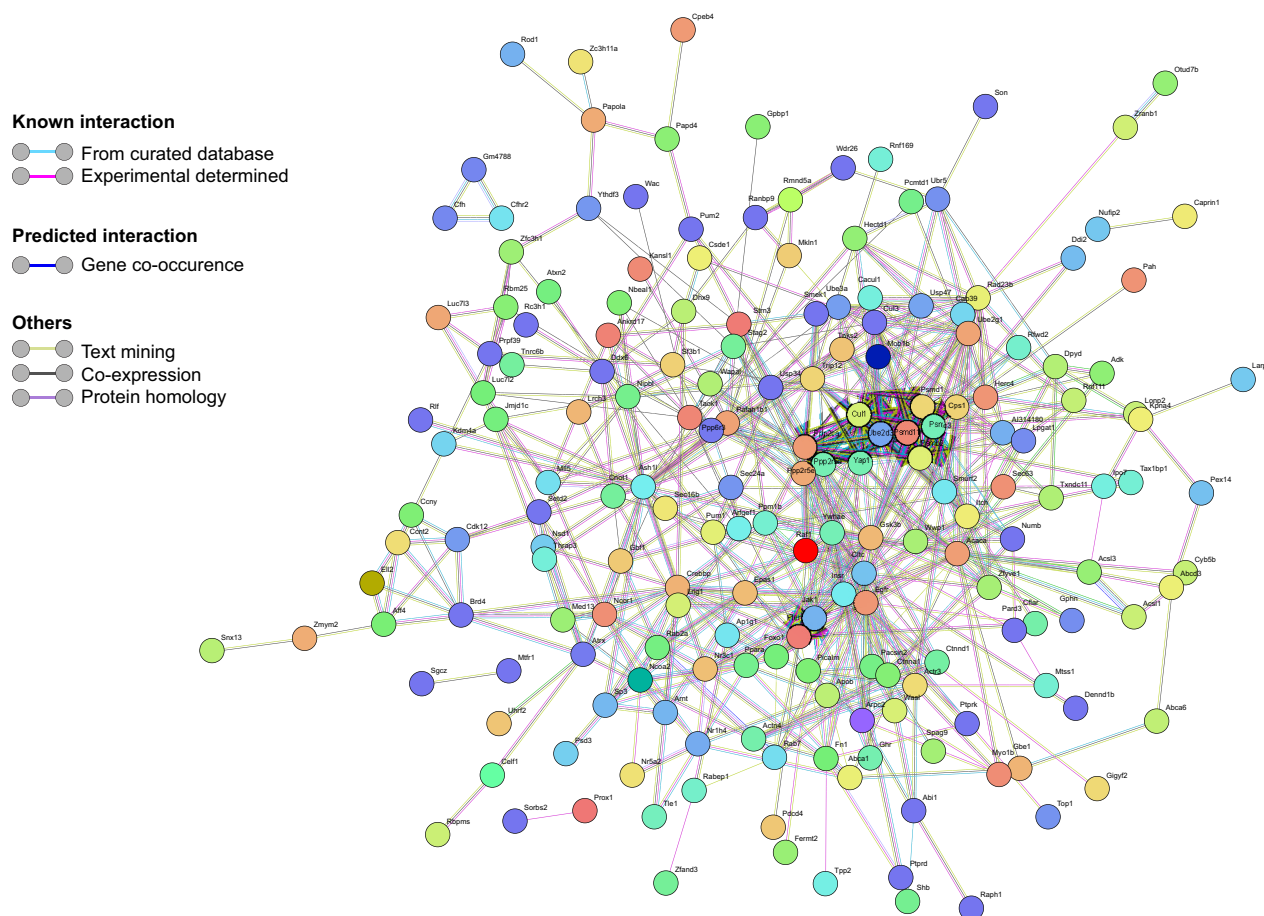


Fig. 6. Most of the *Alb-R26^{Met}*-transposon genes are part of networks of interactions. Projection of *Alb-R26^{Met}*-transposon genes onto the STRING protein-protein interaction network highlights a large network of 179 connected nodes. Associations between 3 genes (1) and 2 genes (3) are also indicated. The colour of the edges corresponds to different types of interactions reported on the left. Nodes not connected (77) are shown in Fig. S6. (This figure appears in colour on the web.)

toocytes carrying an shRNA sequence targeting *Zfand3* as these cells were unable to form tumours (Fig. 8E, Fig. S11A).

Finally, we asked whether these genes were true cooperators, necessitating a primed ‘enhanced RTK’ context, or whether they would act as tumour suppressors on their own. We therefore transfected these shRNA targeting sequences into *immorto-WT* hepatocytes, then performed xenografts in nude mice. Remarkably, shRNA targeting these 16 tumour suppressors failed to confer tumorigenicity to *immorto-WT* hepatocytes (Fig. 8F). Thus, our findings support a model according to which a primed context, such as the one resulting from enhanced RTK levels, is mandatory for manifesting the tumour-suppressive action of these genes following shRNA targeting. As these genes operate in divergent regulatory circuits, our findings illustrate how subtly increased levels of WT RTKs provide a permissive setting to a plethora of deregulated mechanisms for tumorigenesis.

Discussion

Deregulation of RTK signalling is a frequent event in HCC pathology.⁶ Here, to model such deregulation, the context of slightly enhanced MET levels has been employed to identify genetic alterations that accelerate the event of liver tumour

initiation. Studies have been done at stages when tumours in *Alb-R26^{Met}* mice are not present yet (30-weeks old mice) in order to identify the bona fide cooperators of RTKs for liver tumour initiation. The absence of tumours at this stage in *Triple^{tg}* (without enhanced MET levels) enabled us to define the *Alb-R26^{Met}*-transposon genes that acted as cooperators with RTKs rather than as drivers of tumorigenicity. This is further corroborated by our functional validation studies focusing on 15 tumour suppressor candidates, for which we showed that their downregulation confers tumorigenic properties in cells with enhanced MET levels (*immorto-R26^{Met}* hepatocytes), but not in *immorto-WT* hepatocytes. These validation studies also exemplify an extraordinary promiscuous capacity of an RTK such as MET to cooperate with multiple genes engaged in distinct cellular functions, for liver tumorigenesis. Such a large spectrum of cooperativity is further illustrated by our bioinformatic studies, which showed enrichments among identified cooperators of distinct kinases and transcription factors operating in different pathways, as well as enrichment of distinct functions in cells. Thus, once a critical signalling threshold is attained, RTKs such as MET are rather permissive in terms of competence to act together with divergent cooperative inputs in tumorigenesis. Our findings strengthen the role of HGF/MET in HCC and exemplify how elevated MET activity could

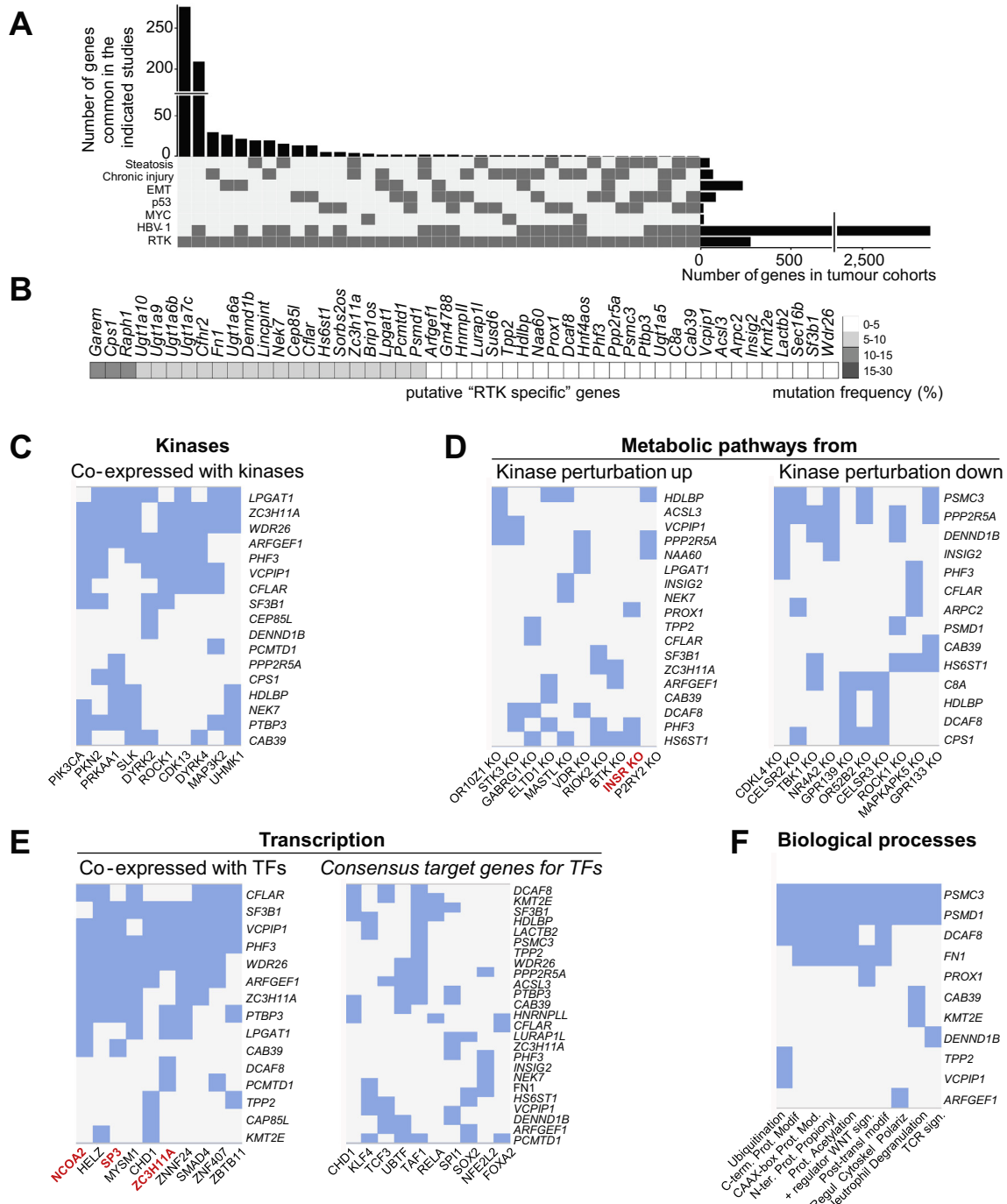


Fig. 7. 'Putative RTK-specific genes' identified in the *Alb-R26^{Met}* genetic setting. (A) Schematic representation reporting the genetic comparison to SB screens performed in other HCC models (steatosis, chronic injury, EMT, HBV, p53, MYC mutant backgrounds).^{21,31-35} Vertical bars: number of *Alb-R26^{Met}*-*transposon* genes overlapping with other studies. Horizontal bars: total number of genes for each screen used for analysis. Dark grey squares: datasets used in each comparison. (B) List of *Alb-R26^{Met}*-*transposon* genes not identified in previous liver transposon studies, named 'putative RTK-specific genes', ordered according to the mutation frequency. (C-F) Enrichment analyses by applying the Enrichr tool. (C) Clustergram reporting the kinases enriched according to their co-expression with 'putative RTK-specific genes' (Coexpressed with kinases, ARCHS4 kinases Coex database). (D) Clustergram reporting kinases recognizable by signatures of gene perturbations (upregulation/downregulation) following kinase knockdown (LINCS L1000 Kinase perturbations up/down databases). (E) Clustergram reporting transcription factors enriched according to either co-occurring (left: Enrichr submission TF-Gene Co-occurrence database) or the consensus targets (right: ENCODE and ChEA consensus TFs from ChIP-X database) with sets of 'putative RTK-specific genes'. (F) Clustergram reporting enrichment of biological processes (Gene Ontology Biological processes database). In D and E, enriched kinases and transcription factors belonging to the *Alb-R26^{Met}*-*transposon* genes are indicated in red. EMT, epithelial-mesenchymal transition; HBV, hepatitis B virus; HCC, hepatocellular carcinoma; RTK, receptor tyrosine kinase; SB, Sleeping Beauty; TF, transcription factor. (This figure appears in colour on the web.)

play an active role at the root of liver tumorigenesis. Notably, increased HGF levels have been reported in patients affected by chronic liver disease, also recapitulated in several animal models

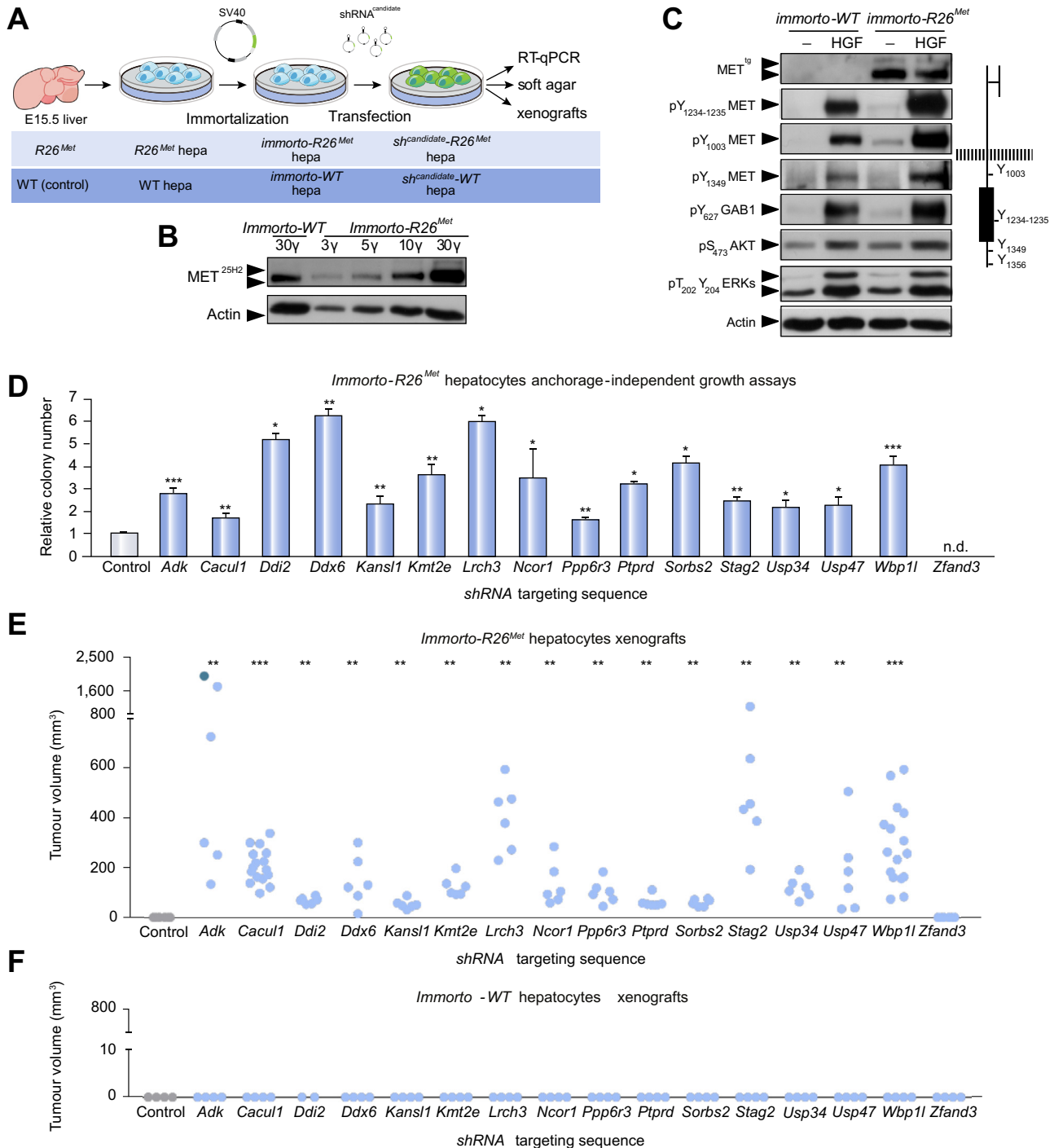
of chronic liver dysfunction, and MET is required during liver regeneration.³⁶⁻³⁸ Thus, in a context of chronic liver disease, an enhanced MET input, while ensuring regeneration, may render

the liver more vulnerable to additional signals, exposing cells to signalling thresholds competent for tumour initiation.

Having identified and functionally validated a set of *Alb-R26^{Met}-transposon* genes, an intriguing issue to explore in future is whether and to what extent these genes represent cooperators of the MET RTK specific to the liver context, or whether these cooperators are also operational for tumorigenesis in other tissues. Our bioinformatic studies show that the *Alb-R26^{Met}-transposon* genes identify different types of cancer among enriched diseases, beside liver cancer. Thus, it is likely that a set of *Alb-R26^{Met}-transposon* genes, when altered, could act as coop-

erators of RTKs in several types of cancers. The *R26^{stopMet}* genetic system offers the possibility of enhancing MET expression in the tissue of choice, according to the tissue-specific Cre employed. Therefore, such a genetic approach will enable the issue of tissue-specificity for qualitative signalling cooperation with RTKs to be addressed in future. This may be particularly relevant in the subset of vulnerable tissues in which a subtle increase in WT MET expression levels is poorly tolerated and in tissues where the MET oncogenic action is well established.³⁹

The comparison we performed between the outcomes of SB transposon mutagenesis carried out in the present *Alb-R26^{Met}*



genetic setting and in other settings^{21,31–35} revealed that among the 275 *Alb-R26^{Met}-transposon* genes, aside from a large group of common hits, 49 genes were only found in the *Alb-R26^{Met}* context, which we named 'putative RTK-specific genes'. For a proportion of them, it is possible that they could have been missed in previous screens because transposon mutagenesis does not reach saturation levels, particularly with small numbers of analysed tumours. Additionally, differences in mouse genetic background, SB transposon versions, sequencing and bioinformatic analyses, can also limit comparisons of genes identified through SB screens.³³ In spite of these limitations, it is tempting to speculate that when altered, at least some of these 'putative RTK-specific genes' may be competent to exert their tumorigenic potential predominantly in a context with enhanced RTK levels (and possibly in few other genetic settings), rather than together with any kind of liver-sensitizing signals. The possibility of such genetic specificity cooperating towards tumorigenesis has recently been proposed through forward genetic screens in mice.^{40,41}

Altogether, the knowledge of these *Alb-R26^{Met}-transposon* genes that we identified in a clinically relevant liver cancer genetic model may contribute to the identification of drivers operating in patients with HCC, as well as genetic interactions with altered RTKs in human HCC. Ultimately, our results will inform the design of new combinatorial therapies for subsets of patients with HCC.

Financial support

This work was funded by INCa (Institut National du Cancer; PLO6_078 and PLBIO12-057), FdF (Fondation de France; 2014_00051580 and 2016_00067080), ARC (Association pour la Recherche contre le Cancer; SFE2011_1203807), and GEFLUC – Les Entreprises contre le Cancer to F.M. Y.F. was supported by the China Scholarship Council (201206350070). S.K.B. was supported by the Higher Education Commission (HEC) of Pakistan – France Campus. M.A. was supported by a FdF fellowship. D.A.L. was supported by an American Cancer Society Research Professorship. AY was supported by grant HA 6905/2-1 of the Deutsche Forschungsgemeinschaft (DFG) and an ERASMUS+ fellowship. The contribution of the Region Provence Alpes Côtés d'Azur and of the Aix-Marseille Université to the IBDM animal facility is also acknowledged. The funders had no role in study design, data col-

lection and analysis, decision to publish, or preparation of the manuscript.

Conflict of interest

The authors declare no conflicts of interest that pertain to this work.

Please refer to the accompanying ICMJE disclosure forms for further details.

Authors' contributions

Y.F.: performed the whole transposon screen and the majority of the experiments; data analysis; provided inputs on the manuscript. S.K.B.: performed the molecular and functional validation of selected candidates. F.D.: performed the majority of the computational work, data analysis, and interpretation. M.A.: performed computational work with human HCC databases and interpretation; provided inputs on studies and on the manuscript. S.R.: generated and characterised *immorto-WT* and *immorto-R26^{Met}* hepatocytes; contributed to functional validation studies of candidate genes. N.A.T.: performed transposon integration data analysis. A.Y.: performed DAVID and KEGG analyses and contributed to computational work using the human HCC cohort from TCGA database. B.H.H.: supervised analyses on DAVID, KEGG, and extraction of human HCC cohort data; provided inputs on the manuscript. R.D.: contributed to establishing the *Alb-R26^{Met}* mouse model; provided inputs on studies and on the manuscript. D.A.L.: provided support for transposon sequencing and computational studies; provided input on writing the paper. F.M.: designed the study, contributed to experimental work, analysed and interpreted data, ensured financial support, and wrote the paper.

Acknowledgements

These results are in part based upon public data generated by TCGA Research Network: <http://cancergenome.nih.gov/>. We are particularly grateful to F. Helmbacher for extremely valuable feedback on the study and for help with improving the manuscript. We thank: Á. M. Martínez-Valverde for providing us the SV40 Large T antigen to immortalize the embryonic hepatocytes; all members of our labs for helpful discussions and comments; V. Girod-David and L. Jullien for excellent help with mouse husbandry.

Fig. 8. Generation of cellular systems for functional exploration of *Alb-R26^{Met}-transposon* genes and functional validations *in vitro* and *in vivo*. (A) Schematic representation of the overall strategy employed for generation of *immorto-R26^{Met}* and *immorto-WT* hepatocytes and their use to assess functionality of *Alb-R26^{Met}-transposon* gene sets. *R26^{Met}* (top) or WT (bottom) livers were dissected from E15.5 embryos and use to established primary embryonic hepatocytes, which were then immortalized with a retrovirus carrying the SV40 Large T antigen. Cells were then transfected with plasmids carrying the shRNA sequence targeting the tumour suppressor candidates. Cells were used for molecular analyses to evaluate the extent of gene downregulation, and for functional studies using anchorage-independent growth (soft-agar) assays and xenografts in nude mice. (B) Quantification and analysis of MET^{TS} vs. endogenous MET levels using protein extracts from *immorto-WT* and *immorto-R26^{Met}* hepatocytes. Note that the MET protein levels present in 10 µg (γ) of total *immorto-R26^{Met}* hepatocyte protein extracts are comparable to those found in 30 µg of control extracts. The anti-MET^{25H2} antibodies recognize both endogenous and MET^{TS} proteins. (C) Western blot analysis of total protein extracts from *immorto-WT* and *immorto-R26^{Met}* hepatocytes before and after HGF stimulation (50 ng/ml). Results show that in these cells phosphorylation of MET on Tyr₁₂₃₄₋₁₂₃₅ (within the kinase domain reflecting MET activity), Tyr₁₀₀₃ (critical for MET protein ubiquitination/degradation), and Tyr₁₃₄₉ (one of the 2 multifunctional docking sites critical for MET signalling^{24,42,43}) as well as of GAB1 on Tyr₆₂₇ is dependent on HGF stimulation. Basal phosphorylation levels of AKT and mitogen activated protein kinases (ERKs) are increased upon HGF stimulation. A scheme summarizing the main tyrosine residues in MET is reported on the right. In B and C, Actin was used as a loading control. (D) Graph reporting the number of colonies formed in anchorage-independent growth assays by *immorto-R26^{Met}* hepatocytes transfected with an shRNA sequence targeting the indicated *R26^{Met}-transposon* genes compared to control cells (either non-transfected or transfected with a shRNA control sequence). Note colony number formation of *immorto-R26^{Met}* hepatocytes with downregulated candidate genes compared with control cells. (E) Quantification of tumour volume in mice injected subcutaneously with *immorto-R26^{Met}* hepatocytes transfected with plasmid carrying the shRNA sequence targeting the indicated gene compared with control cells (either non-transfected or transfected with a control vector). The dark-dot in *Adk* corresponds to a tumour dissected for ethics. (F) Quantification of tumour volume in mice injected sub-cutaneously with *immorto-WT* hepatocytes transfected with plasmid carrying the shRNA sequence targeting the indicated gene compared with control cells (either non-transfected or transfected with a control vector). Note no tumour formation. Significant differences (Mann-Whitney test) compared to controls are indicated on the top. **p* < 0.05; ***p* < 0.01; ****p* < 0.001 (n.d.: not determined). WT, wild-type. (This figure appears in colour on the web.)

Supplementary data

Supplementary data to this article can be found online at <https://doi.org/10.1016/j.jhep.2018.11.027>.

References

Author names in bold designate shared co-first authorship

- [1] Llovet JM, Zucman-Rossi J, Pikarsky E, Sangro B, Schwartz M, Sherman M, et al. Hepatocellular carcinoma. *Nat Rev Dis Primers* 2016;2:16018.
- [2] Zucman-Rossi J, Villanueva A, Nault JC, Llovet JM. Genetic landscape and biomarkers of hepatocellular carcinoma. *Gastroenterology* 2015;149(1226–1239) e1224.
- [3] Cancer Genome Atlas Research Network. Electronic address wbcancer Genome Atlas Research N. Comprehensive and integrative genomic characterization of hepatocellular carcinoma. *Cell* 2017;169, 1327–1341 e1323.
- [4] Llovet JM, Villanueva A, Lachenmayer A, Finn RS. Advances in targeted therapies for hepatocellular carcinoma in the genomic era. *Nat Rev Clin Oncol* 2015;12:408–424.
- [5] Maina F. Strategies to overcome drug resistance of receptor tyrosine kinase-addicted cancer cells. *Curr Med Chem* 2014;21:1607–1617.
- [6] Worns MA, Galle PR. HCC therapies—lessons learned. *Nat Rev Gastroenterol Hepatol* 2014;11:447–452.
- [7] Park WS, Dong SM, Kim SY, Na EY, Shin MS, Pi JH, et al. Somatic mutations in the kinase domain of the Met/hepatocyte growth factor receptor gene in childhood hepatocellular carcinomas. *Cancer Res* 1999;59:307–310.
- [8] **Furlan A, Stagni V, Hussain A**, Richelme S, Conti F, Prodosmo A, et al. Abl interconnects oncogenic Met and p53 core pathways in cancer cells. *Cell Death Differ* 2011;18:1608–1616.
- [9] Kaposi-Novak P, Lee JS, Gomez-Quiroz L, Coulouarn C, Factor VM, Thorgeirsson SS. Met-regulated expression signature defines a subset of human hepatocellular carcinomas with poor prognosis and aggressive phenotype. *J Clin Invest* 2006;116:1582–1595.
- [10] Goyal L, Muzumdar MD, Zhu AX. Targeting the HGF/c-MET pathway in hepatocellular carcinoma. *Clin Cancer Res* 2013;19:2310–2318.
- [11] Giordano S, Columbano A. Met as a therapeutic target in HCC: facts and hopes. *J Hepatol* 2014;60:442–452.
- [12] Horwitz E, Stein I, Andreozzi M, Nemeth J, Shoham A, Pappo O, et al. Human and mouse VEGFA-amplified hepatocellular carcinomas are highly sensitive to sorafenib treatment. *Cancer Discov* 2014;4:730–743.
- [13] Du Z, Caenepeel S, Shen Y, Rex K, Zhang Y, He Y, et al. Preclinical evaluation of AMG 337, a highly selective small molecule met inhibitor, in hepatocellular carcinoma. *Mol Cancer Ther* 2016;15:1227–1237.
- [14] You H, Ding W, Dang H, Jiang Y, Rountree CB. c-Met represents a potential therapeutic target for personalized treatment in hepatocellular carcinoma. *Hepatology* 2011;54:879–889.
- [15] **Genestine M, Caricati E, Fico A**, Richelme S, Hassani H, Sunyach C, et al. Enhanced neuronal Met signalling levels in ALS mice delay disease onset. *Cell Death Dis* 2011;2 e130.
- [16] **Fan Y, Richelme S, Avazeri E**, Audebert S, Helmbacher F, Dono R, et al. Tissue-specific gain of RTK signalling uncovers selective cell vulnerability during embryogenesis. *PLoS Genet* 2015;11 e1005533.
- [17] **Tonges L, Ostendorf T**, Lamballe F, Genestine M, Dono R, Koch JC, et al. Hepatocyte growth factor protects retinal ganglion cells by increasing neuronal survival and axonal regeneration in vitro and in vivo. *J Neurochem* 2011;117:892–903.
- [18] **Fan Y, Arechederra M**, Richelme S, Daian F, Novello C, Calderaro J, et al. A phosphokinome-based screen uncovers new drug synergies for cancer driven by liver-specific gain of nononcogenic receptor tyrosine kinases. *Hepatology* 2017;66:1644–1661.
- [19] Arechederra M, Daian F, Yim A, Bazai SK, Richelme S, Dono R, et al. Hypermethylation of gene body CpG islands predicts high dosage of functional oncogenes in liver cancer. *Nat Commun* 2018;9:3164.
- [20] Uren A, Berns A. Jump-starting cancer gene discovery. *Nat Biotechnol* 2009;27:251–252.
- [21] Keng VW, Villanueva A, Chiang DY, Dupuy AJ, Ryan BJ, Matisse I, et al. A conditional transposon-based insertional mutagenesis screen for genes associated with mouse hepatocellular carcinoma. *Nat Biotechnol* 2009;27:264–274.
- [22] Rahrmann EP, Watson AL, Keng VW, Choi K, Moriarity BS, Beckmann DA, et al. Forward genetic screen for malignant peripheral nerve sheath tumor formation identifies new genes and pathways driving tumorigenesis. *Nat Genet* 2013;45:756–766.
- [23] Furlan A, Roux B, Lamballe F, Conti F, Issaly N, Daian F, et al. Combined drug action of 2-phenylimidazo[2,1-b]benzothiazole derivatives on cancer cells according to their oncogenic molecular signatures. *PLoS ONE* 2012;7 e46738.
- [24] Maina F, Pante G, Helmbacher F, Andres R, Porthin A, Davies AM, et al. Coupling Met to specific pathways results in distinct developmental outcomes. *Mol Cell* 2001;7:1293–1306.
- [25] **Moumen A, Ieraci A**, Patane S, Sole C, Comella JX, Dono R, et al. Met signals hepatocyte survival by preventing Fas-triggered FLIP degradation in a PI3k-Akt-dependent manner. *Hepatology* 2007;45:1210–1217.
- [26] **Furlan A, Lamballe F**, Stagni V, Hussain A, Richelme S, Prodosmo A, et al. Met acts through Abl to regulate p53 transcriptional outcomes and cell survival in the developing liver. *J Hepatol* 2012;57:1292–1298.
- [27] Gonzalez-Rodriguez A, Clampitt JE, Escibano O, Benito M, Rondinone CM, Valverde AM. Developmental switch from prolonged insulin action to increased insulin sensitivity in protein tyrosine phosphatase 1B-deficient hepatocytes. *Endocrinology* 2007;148:594–608.
- [28] Sarver AL, Erdman J, Starr T, Largaespada DA, Silverstein KAT. TAPDANCE: An automated tool to identify and annotate transposon insertion CISs and associations between CISs from next generation sequence data. *BMC Bioinformatics* 2012;13.
- [29] **Guichard C, Amaddeo G, Imbeaud S**, Ladeiro Y, Pelletier L, Maad IB, et al. Integrated analysis of somatic mutations and focal copy-number changes identifies key genes and pathways in hepatocellular carcinoma. *Nat Genet* 2012;44:694–698.
- [30] **Totoki Y, Tatsuno K, Covington KR**, Ueda H, Creighton CJ, Kato M, et al. Trans-ancestry mutational landscape of hepatocellular carcinoma genomes. *Nat Genet* 2014;46:1267–1273.
- [31] O'Donnell KA, Keng VW, York B, Reineke EL, Seo D, Fan D, et al. A Sleeping Beauty mutagenesis screen reveals a tumor suppressor role for Ncoa2/Src-2 in liver cancer. *Proc Natl Acad Sci U S A* 2012;109: E1377–E1386.
- [32] Bard-Chapeau EA, Nguyen AT, Rust AG, Sayadi A, Lee P, Chua BQ, et al. Transposon mutagenesis identifies genes driving hepatocellular carcinoma in a chronic hepatitis B mouse model. *Nat Genet* 2014;46:24–32.
- [33] Riordan JD, Feddersen CR, Tschida BR, Beckmann PJ, Keng VW, Linden MA, et al. Chronic liver injury alters driver mutation profiles in hepatocellular carcinoma in mice. *Hepatology* 2017.
- [34] Tschida BR, Temiz NA, Kuka TP, Lee LA, Riordan JD, Tierrablanca CA, et al. Sleeping beauty insertional mutagenesis in mice identifies drivers of steatosis-associated hepatic tumors. *Cancer Res* 2017;77:6576–6588.
- [35] Kodama T, Newberg JY, Kodama M, Rangel R, Yoshihara K, Tien JC, et al. Transposon mutagenesis identifies genes and cellular processes driving epithelial-mesenchymal transition in hepatocellular carcinoma. *Proc Natl Acad Sci U S A* 2016;113:E3384–3393.
- [36] **Huh CG, Factor VM**, Sanchez A, Uchida K, Conner EA, Thorgeirsson SS. Hepatocyte growth factor/c-met signaling pathway is required for efficient liver regeneration and repair. *Proc Natl Acad Sci U S A* 2004;101:4477–4482.
- [37] Shiota G, Okano JI, Kawasaki H, Kawamoto T, Nakamura T. Serum hepatocyte growth-factor levels in liver-diseases – clinical implications. *Hepatology* 1995;21:106–112.
- [38] Borowiak M, Garratt AN, Wustefeld T, Strehle M, Trautwein C, Birchmeier C. Met provides essential signals for liver regeneration. *Proc Natl Acad Sci U S A* 2004;101:10608–10613.
- [39] **Peacock JD, Pridgeon MG**, Tovar EA, Essenburg CJ, Bowman M, Madaj Z, et al. Genomic status of MET potentiates sensitivity to MET and MEK inhibition in NF1-related malignant peripheral nerve sheath tumors. *Cancer Res* 2018;78:3672–3687.
- [40] Rogers ZN, McFarland CD, Winters IP, Seoane JA, Brady JJ, Yoon S, et al. Mapping the in vivo fitness landscape of lung adenocarcinoma tumor suppression in mice. *Nat Genet* 2018;50:483–486.
- [41] Wangenstein KJ, Wang YJ, Dou Z, Wang AW, Mosleh-Shirazi E, Horlbeck MA, et al. Combinatorial genetics in liver repopulation and carcinogenesis with a novel in vivo CRISPR activation platform. *Hepatology* 2017.
- [42] Ponzetto C, Bardelli A, Zhen Z, Maina F, dalla Zonca P, Giordano S, et al. A multifunctional docking site mediates signaling and transformation by the hepatocyte growth factor/scatter factor receptor family. *Cell* 1994;77:261–271.
- [43] Maina F, Casagrande F, Audero E, Simeone A, Comoglio P, Klein R, et al. Uncoupling of Grb2 from the Met receptor in vivo reveals complex roles in muscle development. *Cell* 1996;87:531–542.